The Stellar Reference Unit for the Europa Orbiter Mission

Carl Christian Liebe
E-mail: carl.c.liebe@jpl.nasa.gov
Telephone: 818 354 7837

Bruce R. Hancock
E-mail: bruce.r.hancock@jpl.nasa.gov
Telephone: 818 354 8801

J. Martin Ratliff
E-mail: j.martin.ratliff@jpl.nasa.gov
Telephone: 818 354 2261

James W. Alexander
E-mail: james.w.alexander@jpl.nasa.gov
Telephone: 818 354 2020

W. John Walker
E-mail: w.john.walker@jpl.nasa.gov
Telephone: 818 354 3260

Allan R. Eisenman
E-mail: allan.eisenman@jpl.nasa.gov
Telephone: 818 354 4999

Jeffrey A. Mellstrom
E-mail: jeffrey.a.mellstrom@jpl.nasa.gov
Telephone: 818 354 0415

Gary M. Swift
E-mail: gary.m.swift@jpl.nasa.gov
Telephone: 818 354 5059

Mark Wadsworth
E-mail: mark.wadsworth@jpl.nasa.gov
Telephone: 818 354 7833

Jet Propulsion Laboratory, California Institute of Technology,
4800 Oak Grove Dr, Pasadena CA. 91109-8099.

Abstract–Star trackers are a reliable and accurate device used by almost all spacecraft in order to autonomously determine their orientation. A star tracker for the future Europa Orbiter Spacecraft poses significant environmental challenges not typically observed in other space missions. The Jovian system in which the star tracker must operate is characterized by extreme intense ionizing radiation, which is primarily due to high-energy electrons and protons trapped by Jupiter's magnetic field. The design of a star tracker that will operate satisfactory in this environment must overcome many challenging problems. Ionizing radiation will cause ordinary optical glass to darken. Silicon based detectors typically experience threshold shifts, increased dark current, reduced quantum efficiency and reduced charge transfer efficiency (in the case of CCDs). An even larger challenge is posed by the proton and electron flux. This is because an electron impinging on a silicon-based detector will typically deposit thousand electron-holes pairs in a pixel and a proton is likely to generate significantly more electron-hole pairs. Electrons and protons incident on any glass in the optical path will generate luminescence and Cerenkov radiation, which degrades the signal to noise ratio. This paper will discuss issues related to the design of a star tracker that can operate in the Europa radiation environment.

TABLE OF CONTENTS

1. INTRODUCTION

Scientific data indicate that Jupiter's fourth largest satellite, Europa, is covered with a surface of ice. Heat generated by Jupiter's tidal pull is believed to produce an ocean of liquid water underneath the ice surface, providing an environment in which life may have evolved. At the Jet Propulsion Laboratory, preparation has begun on a mission to send a spacecraft to Europa in November 2003. The primary scientific objectives will be to measure the thickness of the surface ice and to detect if a liquid ocean does exist [1].

The Europa Orbiter spacecraft will require a star tracker. Typically, a star tracker is an electronic camera connected to a microcomputer. Using a sensed image of a portion of the sky, stars can be located and identified. Thus the orientation of the spacecraft can be determined based on these observations. A modern star tracker is fully autonomous - i.e. it automatically performs pattern recognition of the star constellations in the field of view and calculates the attitude quaternion with respect to the celestial sphere, see Figure 1 [2], [3]. State of the art star trackers typically have a mass of 1-7 kg and consume 5-12 watts of power. Their accuracy is in the arc seconds range [4].

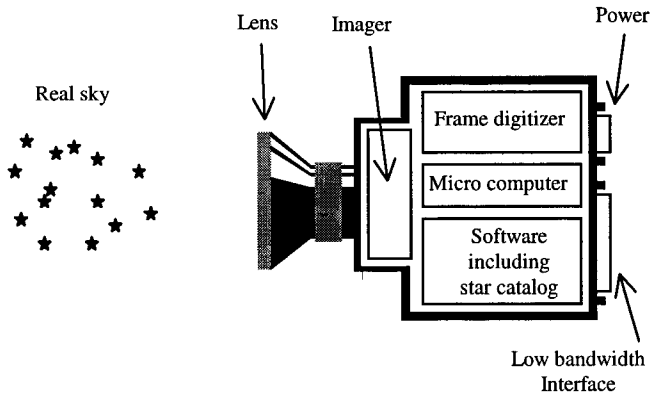

Figure 1. Sketch of a modern star tracker

The radiation environment close to Jupiter poses a unique and significant challenge to spacecraft avionics design. It is estimated that electronics behind a 0.1 inch aluminum shield will receive a Total Ionizing Dose (TID) of 4 MRad(Si). While orbiting Europa, the spacecraft will experience an electron flux of $5.0 \cdot 10^7$ $(cm^2 \cdot s)^{-1}$ for electrons of 1 MeV or greater, and a proton flux of $1.5 \cdot 10^5$ $(cm^2 \cdot s)^{-1}$ for protons of 10 MeV or greater. This is much more radiation than any current star tracker can accommodate[1].

Two sets of requirements are imposed on the star tracker. The first applies to the interplanetary cruise phase from launch until the spacecraft reaches Jupiter. In this phase, the star tracker is exposed to relatively little irradiation. The second set of requirements applies to the orbital phase (first around Jupiter, than Europa), when the star tracker is subjected to the Jovian high radiation environment. The mission at Europa is only planned to last for 30 days.

The Europa star tracker must meet the following requirements over temperature, end-of-life, input supply variation, and radiation environments for each unit. The star tracker may be packaged as more than one physical assembly.

Mass:	< 5 kg
Power consumption:	< 5 Watts
Accuracy[2] (1σ), Yaw, pitch, roll:	< 100 arc seconds
Representative total dose (behind 100 mils Aluminum):	4000 Krad(Si)

Preliminary Cruise Phase Performance Requirements (gyros assumed off):
Update rate: > 1 Hz

Preliminary Mission Phase Performance Requirements (gyros assumed on):
Update rate: > 0.1 Hz

This paper will discuss the issues that are related to operating a star tracker in the Jovian environment.

2. RADIATION ENVIROMENT AT JUPITER

Jupiter, the largest planet in the solar system contains about 71% of all planetary mass in the solar system. The average density of Jupiter is only 1.34 g/cm^3. Based on the density of Jupiter, theoretical models suggest that Jupiter is primarily composed of hydrogen and helium with a small interior core of heavier elements. The high internal pressure in Jupiter converts most of the hydrogen into liquid metallic hydrogen - a good conductor of electricity. Jupiter has a rotational period of 10 hours and this fast rotation combined with convection currents generates a very strong magnetic field. The magnetic field traps charged particles in stable doughnut shaped orbits similar to the terrestrial Van Allan belts [8].

Spacecraft observations by Pioneer and Voyager have made it possible to model the radiation in the Jovian magnetosphere [9]. Particle concentrations present a hazard to spacecraft in a region from about 2.5 R_J (Jupiter radii, with 1 R_J defined as the cloud ceiling) to roughly 15 R_J. Lower concentrations can be found in the outer region of the magnetosphere, which extends to about 100 R_J.

[1] A high radiation environment star scanner and science camera have previously been built for the Galileo spacecraft [5], [6], [7].

[2] Accuracy includes all errors (centroiding error, optics error, NEA etc.) except long-term bore sight stability.

The model can be used to calculate the mission TID because it gives an estimate of the average flux seen over a time interval comparable to the mission duration. Unfortunately, the model makes no estimate of the particle flux at time scales comparable to a star tracker exposure time.

Figure 1 shows the anticipated dose behind various thickness of aluminum shielding [10].

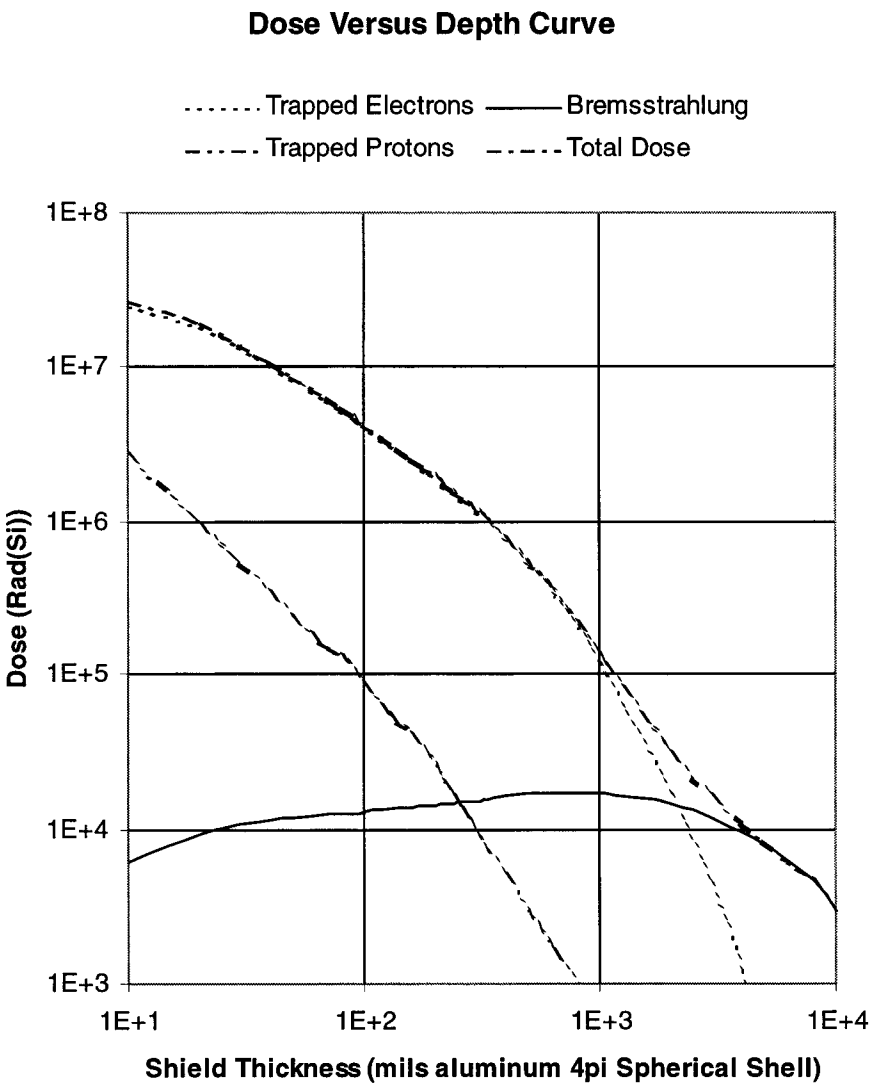

Figure 2. The total dose in Rad(Si) behind various levels of aluminum shielding. Please note that the shielding thickness is given in mils

From Figure 2 it can be seen that bremsstrahlung increases with shielding thickness. This is primarily due to deceleration of electrons in the shielding. The bremsstrahlung radiation is electromagnetic and attenuates exponentially though the shielding. As more shielding is added, the more bremsstrahlung is generated. It is not possible to reduce bremsstrahlung with a reasonable shielding thickness. The spectrum is continuous, consisting largely of soft X-rays but extending into the visible spectrum.

Particles impinging on the detector and the optics in the Jovian environment may cause severe difficulties. The anticipated fluences are shown in Figures 3 and 4. **It is anticipated that the particle flux will pose larger problems than the total dose.** An average flux can be estimated, however, the maximum and minimum flux may vary significantly from this average. The variations can be assigned two categories:

- Predictable flux variations based on trajectory and time. Models for the Jovian magnetosphere have been developed. It is known that the flux depends on the distance to Jupiter, the position around Jupiter etc [9].

- Unpredictable flux variations, such as interaction with the solar wind, statistical variations, and unknown phenomena [11].

The magnitude of the flux variations is unknown at this point. However, if the star tracker should operate continuously, some effort must be put into understanding these variations and designing the star tracker with an appropriate margin.

JPL has performed radiation transportation analyses, to assess the fluence behind various levels of shielding. The fluence is calculated in two cases, 5 g/cm^2 and 15 g/cm^2. Each level of shielding has been calculated using both aluminum and a combination (half-and-half in thickness) of Tungsten and Aluminum as the shield material. The later tends to attenuate the electron fluence more [12].

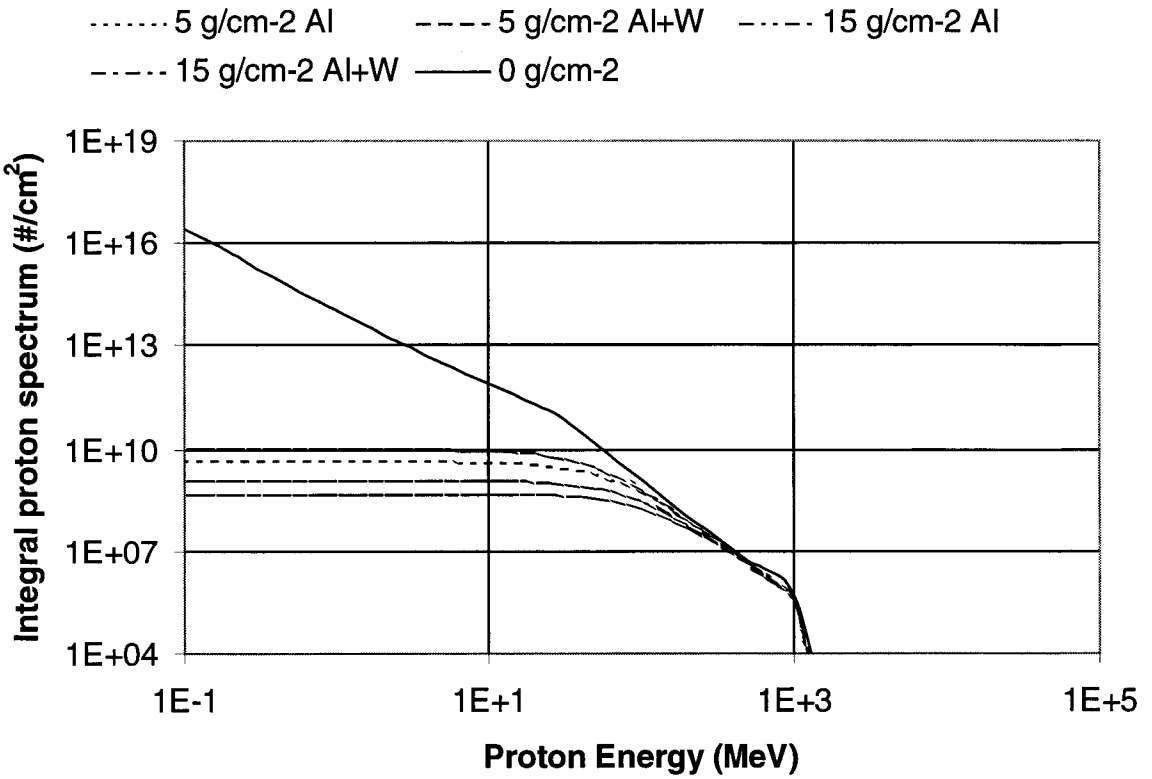

Figure 3. The Integral Proton fluence for the Europa Orbiter mission during 1 month at Europa

3. RADIATION DAMAGE IN THE DETECTOR

This section provides an overview of radiation effects in imaging detectors. It is not intended to be exhaustive in detail, but rather to show the types of effects encountered. It is also aimed towards silicon devices, such as CCDs [13], [14], [15], CIDs [16] and Active Pixel Sensors (CMOS imagers) [17], [18], but should have some applicability to other device types as well [19].

The effects considered here are cumulative, in which the absorption of radiation energy makes permanent changes in the device. All forms of radiation are capable of generating cumulative effects. In these effects, the impact on device performance is determined by the integrated history of radiation exposure. Common measures of integrated exposure include the particle fluence and the Total Ionizing Dose (TID). It must be emphasized that these effects may also depend on other factors, such as temperature and bias conditions. Furthermore, the effects may change with time, e.g. through annealing or migration of defects.

Ionization Damage

Ionization occurs when the absorbed radiation energy goes into forming electron-hole pairs. Ionizing dose is normally measured as the energy absorbed per unit mass of material, with 1 rad defined as 100 erg/g. Because of the details of the interaction physics, the dose per unit of fluence depends on the type and energy of radiation, and on the substrate material. In order to account for this last effect, values of ionizing dose must be referenced to a particular material, e.g. rad(Si). In silicon, one electron-hole pair is formed for every 3.7 eV absorbed.

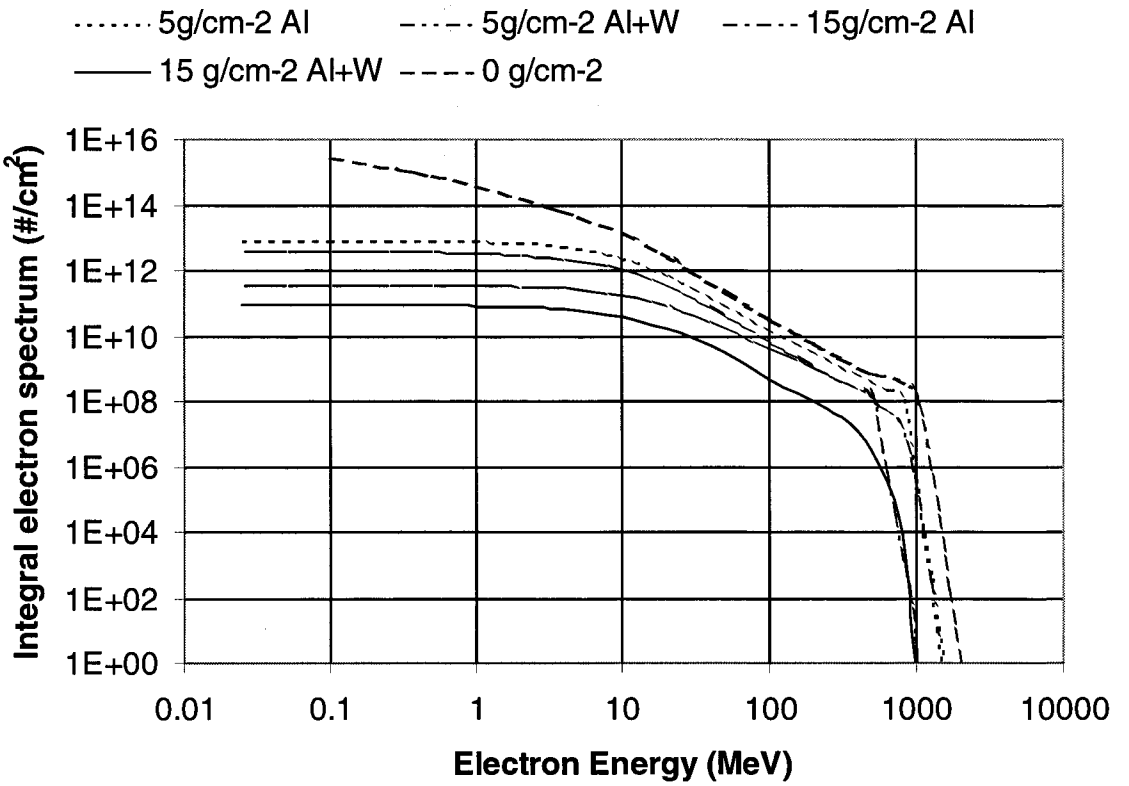

Figure 4. The integral electron fluence for the Europa Orbiter mission during 1 month at Europa

Generally, ionization causes problems only in insulators, notably field oxides and gate oxides on silicon MOS devices. Electron-hole pairs affect device characteristics through trapping of carriers (usually holes), or interactions of carriers with bonding electrons, particularly at interfaces. These effects are highly dependent on the microscopic structure of the insulator, which in turn depends on processing details. Therefore, the sensitivity to ionizing dose can vary enormously from one manufacturer to another, and even from one lot to another for a given manufacturer.

Electron-hole pairs generated by radiation may recombine, rendering them harmless. Some, however, do not and the fraction that survives is known as the charge yield. The charge yield depends on the electric field, the ionization track density, and to some extent the temperature. In particular, high electric fields, high particle energies and low mass particles (i.e. electrons and secondary electrons produced by photons) produce high charge yields. As a result, *bias, radiation type, and energy* can significantly affect the amount of damage for a given ionizing dose.

Trapping of carriers and transport of carriers to interfaces also depend on temperature and electric fields. This can lead to annealing effects. In general, high temperatures can release trapped carriers, but often enhance their transport to interfaces where other damage may occur.

One of the major effects of radiation on MOS devices is a threshold voltage shift. This result from two causes, the trapping of holes in the oxide and the formation of charged interface states. Hole trapping, which dominates at low doses, results in a negative shift in threshold voltage tending to turn n-channel MOSFETs on and p-channel MOSFETs off. Interface states, on the other hand, are negatively charged in n-channel devices and positively charged in p-channel devices, resulting in positive and negative contributions to the threshold shift, respectively.

Threshold shifts usually increase linearly at low doses, slowing or saturating at higher doses. In n-channel MOSFETs they may even reverse, as interface states become dominant. Annealing can release some of the trapped holes, shifting the threshold in a positive direction. In n-MOSFETs the net threshold shift after annealing may even be positive, an effect known as rebound. Interface states can not be annealed at practical temperatures.

Threshold shifts depend on many parameters, including *oxide quality, thickness, and device type*, and are subject to effects of temperature, bias and radiation type, as described above. A common model predicts that the threshold shift is proportional to the square of the oxide thickness, making thicker oxides, as found in older processes, more susceptible. Furthermore, threshold shifts are usually larger for p-channel devices than for n-channel devices. Threshold shifts range from less than 1 mV/KRad for advanced

radiation hard processes, to more than 100 mV/KRad for some CCDs.

In analog circuits threshold shifts can result in improper bias conditions, while in digital circuits it results in degraded timing and noise margin and increased power consumption. Sufficiently large threshold shifts result in functional failure.

Threshold shifts may also occur under the field oxide that separates devices. If this threshold reaches zero (typically between n-channel devices) an inversion layer will form, destroying the isolation and shorting out the devices. This is a common source of failure for devices in non-radiation hardened processes.

Finally, threshold shifts may result in an inversion region connecting n-channel sources and drains along the gate oxide to field oxide transition, or "birdsbeak". This produces leakage current that can be very serious in the charge sensitive applications found in imaging. Likewise, it can destroy the isolation between CCD pixels.

The second major effect of ionizing radiation is the increase of the surface generated/recombination rate due to the formation of interface states. These are energy levels within the bandgap of the silicon, located at the silicon-oxide interface, so that they can communicate with the carriers in the silicon. Wherever interface states are in a depletion region, they result in electron-hole pair generation, leading to dark current and leakage.

Surface generated dark current is a serious problem for imaging, where it may exceed the signals to be detected. Even when it is less than the signal, temporal and spatial variations may contribute a very serious noise component. In MPP CCDs and CIDs the problem is mitigated by surface pinning, which prevents a depletion region from forming at the silicon-oxide interface under the integrating phase. However, surface generation still occurs under the other phases, through which the signal charge must pass. Surface generation in non-MPP devices is typically of the order of 1 nA/cm^2/krad at room temperature.

When interface states are not in a depletion region, as in a photodiode, they can instead result in recombination of carriers. *The greatest problem with this is* for carriers generated near the surface, i.e. by strongly absorbed blue light. Thus the increase in interface state density with radiation degrades the blue response of photodiodes.

Like hole trapping, interface state formation is strongly process dependent. It is also subject to important temperature effects. At low temperatures, interface state formation is inhibited. Under annealing conditions, as trapped holes diffuse to the interface, the interface state density may increase significantly. However, this "reverse annealing" applying a negative gate bias during annealing may inhibit effect, well demonstrated in CCDs.

Displacement Damage

The second category of cumulative damage is displacement damage, which occurs when silicon atoms are displaced from the crystal lattice. This, in turn, results in vacancies and interstitial silicon atoms, which can produce energy states within the bandgap. The production of displacements is an inherent property of radiation and the silicon crystal, making it relatively technology independent. However, many of the energy states involve vacancy-impurity complexes. This makes displacement damage somewhat dependent on technology (e.g. the selection of dopants), but unlike ionization effects, relatively insensitive to process details (e.g. processing temperatures).

In order to create displacements, the radiation must impart both energy and momentum to silicon atoms. This makes low-mass particles (electrons and especially photons) inefficient at producing displacement damage. In a space environment, most displacement damage usually comes from protons, though electrons and even gamma rays can also produce displacements. Neutrons are also very effective at producing displacements, as are heavy ions. However, these are found in smaller numbers.

Displacement cross sections are a function of energy, peaking at low energy (~10 keV for protons) and decreasing approximately as 1/E at higher energies. This differs from the behavior of the ionization cross section, which peaks at a higher energy, and has a slightly weaker falloff at high energies. The ratio of displacement to ionization is not constant, but is a decreasing function of energy, with most rapid changes below ~100 keV for protons.

As a result of this energy dependence, displacement damage does not track ionizing dose, even for a given radiation type, but depends on the energy spectrum. Between different types of radiation there may be orders of magnitude difference. The appropriate measure of displacement dose is generally considered to be the energy absorbed by the nuclei, as opposed to electrons. This may also be measured in rads, but it must be carefully distinguished as the displacement dose, since it is usually several orders of magnitude smaller than the ionizing dose.

Displacement damage is generally independent of bias, and is only weakly dependent on temperature, although the formation of certain complexes (e.g. phosphorus-vacancy of P-V) is inhibited at low temperatures. Unlike threshold shifts, displacement damage cannot be annealed at practical temperatures. However, although the damage itself is not strongly dependent on bias or temperature, the device effects typically are.

As with interface states, the mid-gap energy levels associated with displacement damage can act as generation or recombination sites. When they are in a depletion region they act as generation sites, producing dark current. The dark current depends in an Arrhenius fashion (approximately exponentially) with temperature, with activation energy approximately half the bandgap. Because the volume of the depletion region increases with bias, the dark current does also. Additionally, it is believed that mid-gap states in high

field regions can have their current generation capacity greatly amplified. This is sometimes given as the explanation of "hot pixels", with very high dark current, in proton irradiated CCDs and CIDs.

When mid-gap states are outside a depletion region they act as recombination centers, reducing the diffusion length. This inhibits the collection of carriers generated deep within the silicon, i.e. by weakly absorbed red light. The diffusion length, L_d is generally considered to depend on the fluence Φ as $1/L^2 = 1/Lo^2 + K\Phi$, where K depends on the radiation type and energy.

In addition to acting as generation-recombination sites, states within the energy gap may act as trapping centers, temporarily holding carriers and releasing them later. This is a problem in CCDs, where it can delay the shifting of charge from one pixel to another, reducing the charge transfer efficiency (CTE). Because the release of trapped charge is an Arrhenius process, it depends on the temperature and on the energy of the particular mid-gap state. The CTE also depends on the clock timing and on the charge packet size.

Analysis and testing conditions.

In analyzing or testing devices for radiation environments there are several factors that must be considered carefully.

For ionizing dose effects:

- Ionizing dose effects are very process-sensitive. Don't assume one manufacturer's results can be applied to another.
- Ionizing dose effects depend on the type and energy of the radiation. This can produce differences of a factor of ~2.
- Be sure to consider the effects of bias and temperature, both during and after irradiation.
- Beware of annealing effects on interface state densities.

For displacement damage effects:

- Displacement damage effects are enormously dependent on radiation type and energy. Testing with photons (X-ray, gamma ray) will seriously underestimate these effects.
- Displacement damage effects do not necessarily track the ionizing dose.

4. PARTICLES IMPINGING ON THE DETECTOR

Transient effects come from the momentary presence of electron-hole pairs produced by ionizing radiation. Collection of one or the other of these carrier types places an (approximately) instantaneous charge on some node of a circuit, impacting the operation of the circuit.

A common model for transient effects assumes that any charge generated within a certain volume will be collected. As a particle passes through a device it generates a charge track, with a density given by the electronic stopping power for that particle divided by the pair production energy (3.7 eV for silicon). The track density and length of the track in the sensitive volume then determine the charge deposited. Because slower, more highly charged particles create denser charge tracks, heavy ions are particularly effective at producing transient charge. For transient effects, stopping power is usually measured by the LET (Linear Energy Transfer), in units of MeV/mg/cm^2 or MeV/cm (the first multiplied with the density, 2.3 g/cm^3 for Si). Figure 5 shows the LET for protons and electrons in silicon [20], [21].

As an example, assume that a pixel looks like the simplified sketch in Figure 6 below.

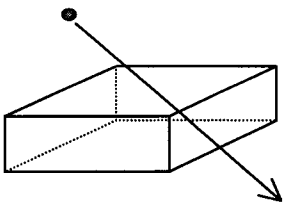

Figure 6. Particle impinging on a pixel in a silicon based detector

Assume that the dimensions for the pixel in a silicon based detector are 12 μm x 12 μm, and the thickness of the sensible volume is 10 μm (approximately the epitaxial layer thickness of a chip). We assume that the particle trajectory is a straight line. This is not entirely true, but can be used with good approximation. Based on Gauss theorem, it is possible to show that for any concave object, the average path length is:

$$Average\ Path\ Length = \frac{4 \cdot Volume\ of\ Object}{Surface\ Area\ of\ Object}$$

The average path length for a particle impinging on the simplified pixel would then be 7.5 μm.

As an arbitrary example, say, the particle is an electron with energy of 1 MeV. At this energy, the LET is 3.8 MeV/cm. Hence, the electron deposits 7.5μm·3.8MeV/cm = 2.8KeV. Each electron hole pair generated requires 3.7 eV in Silicon. This is equivalent to ~750 electron-hole pairs.

Another arbitrary selected calculation can also be done if the impinging particle is a proton. Say, it is a 200 KeV proton. The LET is 445 MeV/cm. The range for protons at this energy is 1.8μm and therefore will the entire energy be deposited in this distance. Each electron-hole pair in silicon requires 3.7 eV. The proton will generate approximately 54000 electron-hole pairs.

It can not be emphasized enough how serious this problem is. The two above random calculations only shows the magnitude of a charged particle impinging on the detector. The fluences of charged particles were shown previous. As discussed later, it is impossible to determine a star centroid in the vicinity of a proton hit. Electron hits will add noise to the star centroid position estimates.

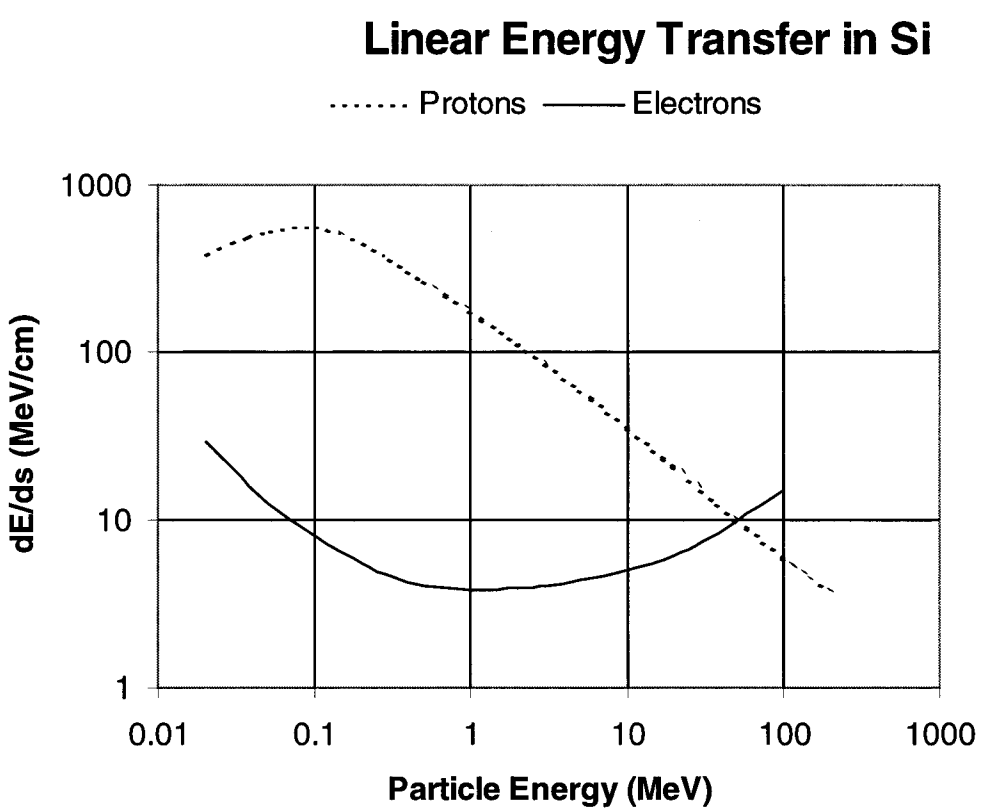

Figure 5. The LET versus particle energy for electrons and protons

Upset

Upset occurs in digital circuits when the radiation-induced charge changes the logical value of a signal. Most often, the term is applied to the situation when the value in a register (i.e. the state of a flip-flop) is changed. Assuming that there is some minimum charge required upsetting a flip-flop, there will likewise be some minimum track density or LET required. Susceptibility to upset is usually described by a threshold LET and a saturated cross section, the maximum cross section achieved at high LET. From these two numbers, and an environment, the upset rate can be computed.

The Europa Orbiter project requirements for parts SEU acceptability are either: 1) No upsets to an effective LET = 75MeV/mg/cm^2 at a fluence of 10^7 ions/cm^2 or greater. 2) Calculation of a device's upset rate shall be equal to or less than the required circuit upset rate (if available) or the default rate of 10^{-10} upset per bit per day.

Upsets can also occur as transient pulses generated by deposition of charge on logic lines. These are most troublesome on clock lines. Additionally, the same sort of situation can occur on analog signals. In that case, the effects are similar to interference effects.

Latchup

Latchup occurs in non-SOI CMOS devices because of the parasitic npn and pnp bipolar transistors that are always present. These parasitic transistors are in a positive feedback configuration. Under normal conditions the operating currents are very low and the loop gain is less than one, hence they cause no problems. However, the charge deposited by a transient event can raise the current level and therefore the loop gain so that a runaway situation occurs. Then large currents are drawn, usually shorting the power supply. Latchup generally does not clear itself and can be destructive. Like upset, a threshold LET and a saturated cross section describe latchup.

5. DARKENING OF GLASS

Ordinary glass darkens due to irradiation. Typically glasses begin to darken after a few KRads of irradiation. The transmission initially decreases in the short wavelengths and then progressively decreases at longer wavelengths, as the glass is irradiated [5].

The darkening of the glass is proportional to the number of certain impurities, called color centers present in the glass. The optical properties of these color centers change when they get ionized [5]. The color centers also anneals with a rate, which is a function of the temperature. The transmission of a piece of glass at a given time therefore depends on both the dose rate and the temperature [22].

One way to minimize darkening of glass is to add cerium oxide, which minimizes the color center generation. High purity synthetic fused silica is resistant to darkening. One manufacturer claims no visible change in optical transmission at the following exposure levels [23], [24]:

Dose (Rad(Si))	Radiation	Energy
$6.3x10^{16}$	Electron	800 kV
$1.4x10^{7}$	Electron	1.5 MeV
10^{10}	Gamma	1 MeV
10^{8}	Proton	2 MeV
10^{20}	Neutrons	Neutrons/cm^2

6. PARTICLES IMPINGING ON THE OPTICS

Particles impinging on optics result in a "glow", and may represent a problem in the Europa star tracker if not carefully included in the design. There are two phenomena associated with impinging particles in the optics: luminescence and Cerenkov radiation.

Luminescence:

When energy is absorbed by any kind of matter, photon emissions may be the result. If the absorbed energy does not increase the thermal energy stored in the material, but changes its excited state, the emissions of photons is called luminescence.

Luminescence can be divided into two different categories, fluorescence and phosphorescence depending on the time delay for the photon emission. If the photons are emitted less than 10 nano seconds after the excitation the luminescence is called fluorescence, otherwise it is called phosphorescence. The emissions can be delayed for hours because the transition to the initial stage is going though a meta-stable state.

It is difficult to make an analytical model for the faction of the deposited energy that is transformed into heat, displacement damage, luminescence etc. Therefore, experimental results must be used to assess the effect. As an example [25] has published the following results, valid in the spectral band of 320-570 nm:

Glass type	Luminescence Photons/(100nm·MeV) in 4π sr.
Al_2O_3, Sample 1	533
Al_2O_3, Sample 2	386
Al_2O_3, Sample 3	115
Al_2O_3, Sample 4	890
Al_2O_3, Sample 5	125
Spectrosil	40
7940 glass	35
Suprasil	40
8337 glass	67
9741 glass	75
7056 glass	35

The following example shows how a crude assessment of the luminescence can be made. Assume that a lens made of Suprasil is a cylinder with a diameter of 4 cm and height of 5 cm. The lens is exposed to the Jovian environment with no shielding.

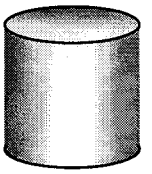

Figure 7. Simple example to assess luminescence. The Suprasil cylinder is 4 cm in diameter and 5 cm in height

This lens has a surface area, S = 87.9 cm^2 and a volume, V = 62.8 cm^3. Utilizing the average path length formula, from previous paragraph, gives an average path on ~2.8 cm. Determining the total energy deposited in the lens is done by integrating over the particle fluxes times the particle energies. The total energy is used for all particles with ranges less than the average path. Particles with ranges longer than the average path does not contribute much to the result, since there are few of them. The total energy deposited by electrons and protons are calculated to be $1.45 \cdot 10^{11}$ MeV/s. It is assumed that the detector is sensitive from 400 nm to 750 nm. [25]'s data are only valid in the band of 320-570 nm, but we assume that it can be used to 750 nm. Suprasil generates on the average 40 photons/(100nm·MeV). Therefore 40 photons/(100nm·MeV) ·3.5(100) nm·$1.45 \cdot 10^{11}$ MeV/s = $2.0 \cdot 10^{13}$ photons/s will be generated in the lens at the detector sensitive wavelengths. These photons are emitted in all directions (4π sr).

Cerenkov radiation:

Cerenkov radiation is generated by charged particles with a velocity that is greater than the speed of light in the glass. Although, no particle can travel faster than the speed of light in vacuum, in glass with an refractive index n, a particle may travel faster than speed of light if v > C/n [26], [27].

If we assume that the refractive index is n = 1.4, then this only affects electrons with energies larger than 220 KeV and protons with energies larger than 400 MeV.

Cerenkov radiation is only emitted during the deceleration, and is emitted along the surface of a forward-directed cone aligned with the particle velocity vector. The wavelength of the light is mainly in the UV/blue end of the spectrum. It can be shown that the half angle of the cone is $\cos\phi = \beta'/\beta$. Where β is the velocity of the particle and β' is the velocity of light in the glass.

The Cerenkov radiation caused by electrons will have to be included in the design considerations for the Europa star tracker.

7. ALGORITHM DESIGN

The star tracker—referring to both the star tracker hardware and software—must work together in both the Europa environment, and in the relatively benign inter-planetary cruise phase. During the cruise phase, the star tracker will be used without gyros, and thus must provide full attitude information at 1Hz or faster to meet requirements using standard star tracker algorithmic approaches [28]. This section discusses the algorithmic challenges. In the vicinity of Europa, many difficulties arise for algorithms. The baseline is to always have an inertial reference unit (IRU) providing high rate attitude updates, so that the algorithms are not required to provide high rate updates. The problems discussed below primarily affect detectors such as CCD's, APS's, and CID's. There are other detector technologies that may perform differently. To illustrate the radiation effects more concretely, examples are given for a 512 by 512 pixel CCD, with 20μm x 20μm pixels, and with a 10 μm epitaxial layer. We also assume that a 5'th magnitude star induces 25,000 electrons/second on the detector, distributed over a five by five pixel region.[3]

The key problems for algorithm design are (1) luminescence (including Cerenkov and other photon producing radiation processes) and glass darkening, (2) high energy electrons and other particles depositing energy on the focal plane, producing electron-hole pairs, and finally (3) degradation of the detector. Each is discussed separately below. One of the major trades to be made is reflective versus refractive elements in the optical path.

Refractive designs can provide large fields of view, thus allowing the use of brighter stars. However, with refractive elements comes luminescence and Cerenkov. Luminescence and Cerenkov adds background signal, proportional to the image exposure time. It is expected that the added background will vary smoothly over the focal plane, so that the contribution to a given pixel is nearly the same as its neighbors. Detecting and measuring a star against the background depends on the signal and noise, where the signal is the star signal, and the noise, which includes the noise of the luminescence (which is the square root of the signal), along with other noise sources. For low level background signals, the main effect that add noise is photon statistics; as example, a contribution of 10,000 electrons/pixel adds only 100 electrons of noise/pixel. Assuming twenty-five pixels involved in a centroid computation, the total signal-to-noise ratio is approximately 19.6 for a sixth magnitude star and one second integration. At higher levels, the pixel non-uniformity provides the dominant effects. With a typical 2% to 3% RMS pixel-to-pixel response variation, the same 10,000 electron background causes a 200 to 300 electron bias. As the background level increases, the pixel response variation becomes an even larger contributor. Of course, if the luminescence is significantly higher, saturation results, making all measurements impossible. One way to reduce the effects of pixel-to-pixel variation is to calibrate (not a trivial task) the individual pixel responses, or to provide real-time background estimates on a pixel by pixel basis. Glass darkening is not expected to be a significant problem with modern glasses, if the system is defined for end-of-life performance.

Particle impingement adds noise electron-hole pairs to a detector, the amount and distribution depends on the stopping power of the detector material, the thickness of the sensitive area, the angle of incidence and the energy of the particle. Electrons can deposit thousands of signal electrons into a detector. Heavier particles such as protons deposit significantly larger signals. Fortunately, this effect is transitory, lasting only for one frame. If a proton strikes near (say 3 pixels) from a star, measurement and detection may be impossible for that star. In the Europa environment, heavy particles are not expected to be a big problem with careful algorithm design. Behind shielding, heavy particles are expected to be orders of magnitude lower than the electron flux, which is expected to be the main problem for star measurement. During typical Europa operation, we are anticipating in the range of one million electrons/second to hit the detector. On the average, each 5x5 centroid area would receive 100 high energy electrons/second, and a contribution (on the average) of 150,000 non-uniformly distributed signal electrons/second, compared to the 25,000 expected for a 5'th magnitude star. This electron flux can clearly cause a centroid bias, or a detection failure. There are some ways to reduce the effect, such as using only bright stars in selected fields (which has a big impact on the whole S/C operation), or more, smaller pixels with a smaller star image. The most obvious solution approach would be to limit the rate that signal can be accumulated (either on the detector, or by using high sampling rates), since photons from a star arrive essentially at constant rate, whereas particles provide infrequent "instantaneous" charge depositions.

The star tracker design must eliminate failure effects such as significant CTE loss in CCD's must be included in the detector selection. Dark current spikes (bright pixels) will also be a problem, and can be addressed by either operation at cold temperatures, or possibly by somewhat complicated algorithm design. Since "spikes" are persistent, there is the possibility of locating and keeping track of the most significant ones. However, the transient radiation, star images, and luminescence complicate the algorithms. Finally, the star tracker algorithms can make use of the attitude information provided by the IRU to propagate frame to frame attitudes. During initialization the star tracker can acquire multiple frames, and compare the spots found on one frame to other frames by using the IRU provided relative attitude information.

[3] In star trackers the image is defocused on purpose, to increase the accuracy [29].

Finally, even when a star tracker design meets the typical Europa requirements, there may be short period of time that the flux becomes too high, since the electron/proton flux rate is expected to vary significantly. Part of the star tracker algorithm design is to then determine when tracking or initialization is failing due to high flux rates; this determination can be used by S/C fault protection to rely only on gyros, turn to very bright star fields, or S/C safing.

Summarizing, there are many problems in the SRU hardware and algorithm design. The trades in hardware versus software solutions, cost, mass, power, and reliability have not yet been done, and will require careful study.

8. SUMMERY

The star tracker for the Europa Orbiter Mission has been discussed in this paper. No existing star tracker design can be used, because of the intense radiation environment at Europa.

The requirement of withstanding 4 MRad(Si) behind 100 mils of aluminum shielding is challenging because the mass of the star tracker (including shielding) must be kept below 5 kg. This means that any glass potentially used in the optical path, the detector itself and electronics should be able to withstand a significant dose.

The largest problem facing the Europa Orbiter star tracker is considered to be the flux of charged particles while at the 30 days mission at Europa. It is expected that half of the total dose will be received during this short period.

The charged particles impinging on the optics will make a "glow" in the optics. This is due to Cerenkov radiation and Luminescence. It is expected that this glow will be uniformly over the focal plane and only have a moderate noise component. However, due to the non-uniformity of pixels this phenomenon will have to be taken into consideration.

The charged particles impinging on the detector is the real challenge. A proton impinging on a pixel is likely to cause a bright spot. Fortunately, moderate shielding will remove most protons. Electrons impinging on the image detector are more severe. An electron impinging on a pixel will typically deposit 1000 electron hole pairs. The electron flux is orders of magnitude larger than the proton flux behind moderate levels of shielding. It is difficult to detect if an electron has hit a pixel. This is one of the core problems, when designing the star tracker and the algorithm.

This paper has been discussing the issues related to operating a star tracker in the Europa environment. At this stage, no design or detector has been selected for the spacecraft.

9. ACKNOWLEDGEMENT

The authors would like to thank Dr. Curtis Padgett for review and comments on this paper. Dr. Robin W. Evans provided the radiation transport analysis.

The research described here was carried out at the Jet Propulsion Laboratory, California Institute of Technology, and was sponsored by the National Aeronautics and Space Administration. References herein to any specific commercial product, process or service by trademark, manufacturer, or otherwise, does not constitute or imply its endorsement by the United States Government or the Jet Propulsion Laboratory, California Institute of technology.

10. REFERENCES

[1] http://www.jpl.nasa.gov/ice_fire//europao.htm.
[2] C.C.Liebe: Pattern Recognition of Star Constellations for Spacecraft Applications, IEEE AES Magazine. June 92, p. 34-41.
[3] A.R. Eisenman, C.C.Liebe: The Advancing state-of-the-art in Second Generation Star Trackers, Proceedings of IEEE Aerospace conference, Aspen 1998, fp241.pdf.
[4] A.R.Eisenman, C.C.Liebe, and J.L.J¢rgensen: The New Generation of Autonomous star trackers, SPIE Proceedings, Vol. 3221, 1997, p. 524-535.
[5] M.M.Birnbaum et al: Development of a Radiation-Hard Photomultiplier Tube, AiAA Guidance and Control Conference, AiAA-84-1852.
[6] M.M.Birnbaum et al: A radiation-Hardened Star scanner for Spacecraft Guidance and Control, Journal of Guidance, Control and Dynamics, Volume 6, Number 1, Jan-Feb 1983, p. 39.
[7] K. P. Klaasen et al: Charge coupled device television camera for NASA's Galileo mission to Jupiter, Optical Engineering, 23(3), 334-342 (May/June 1984).
[8] Michael A. Seeds: Horizons, Exploring the Universe, Wadsworth Publishing Company, 1998, ISBN: 0-534-52434-6.
[9] N. Divine, H.B. Garrett: Charged Particle Distributions in Jupiter's Magnetosphere, Journal of Geophysical research, Vol. 88, No. A9, p 6889-6903, Sep. 1983.
[10] T.W.Larson: Preliminary X2000 First Delivery Project, Environmental Design and Test Requirements, May 29, 1998, Jet Propulsion Laboratory, JPL D-15517. JPL Internal Document.
[11] Robert Bunker: Galileo Star Scanner Performance at JOI, 11/11/93. Presentation at JPL. JPL Internal Document.
[12] Dr. Robin W. Evans, Radiation Transport Though a Generic Stellar Reference Unit for the X2000 spacecraft. JPL Interoffice Memorandum 5052-98-135. JPL internal document.

[13] P.A.Bates et al: Radiation hardened, Backside illuminated 512 x 512 Charge Coupled Device, SPIE Vol. 2415, p. 43 – 57.
[14] G.R.Hopkinson et al: Proton Effects in charge-Coupled Devices, IEEE Transactions on nuclear Science, Vol. 43, No 2, April 1996, p. 614 – 627.
[15] J.P.Spratt: The effects of nuclear Radiation on P-channel CCD Imagers, 0-7803-4061-2/97, 1997 IEEE.
[16] J. Carbone et al: New CID Detectors/Cameras for use in ionizing radiation environments, Proceedings, 43rd Conference on robotics and remote systems, 1995, p.43-50.
[17] Bruce Hancock, Radiation Effects in CCD and APS Sensors, A Comparative Overview, 7/31/97, *presentation at JPL, Internal document.*
[18] E.R.Fossum: Active Pixel Sensors: Are CCD's dinosaurs? *Proc. of the SPIE Vol. 1900, Charge-Coupled Devices and solid State Optical sensors III* (1993).
[19] J.G.Timothy, R.L.Bybee: Effect of 1MeV gamma radiation on a multi-anode microchannel array detector tube, Rev. Sci. Instrum. Vol. 50, No. 6, June 1979, p.743 – 746.
[20] T.P.Ma, Paul V. Dressendorfer: Ionizing Radiation effects in MOS devices and Circuitry, John Wiley and Sons, New York, p. 93.
[21] James Janesick: CCD Radiation Working Group 3, Jet Propulsion Laboratory, Sep 30, 1991.
[22] Private communications with Dr. Charles E. Barnes, Jet Propulsion Laboratory.
[23] Data sheets from Heraeus Amersil, Inc, 3473 Satellite Blvd., Duluth, GA 30096-5821, Suprasil.
[24] Paul B. Willis: Summary of Findings: Materials selection for the X-2000 Mission. Jet Propulsion Laboratory, Interoffice memorandum, September 28, 1998, Iom number: 352h-98-061. JPL internal document.
[25] W. Viehmann et al: Photomultiplier window materials under electron irradiation: fluorescence and phosphorescence, Applied Optics, Vol. 14, No. 9, p. 2104-2115. Sep. 1975.
[26] http://www.nuc.umr.edu/~ans/cerenkov.html.
[27] http://zebu.uoregon.edu/~js/glossary/cerenkov_radiation.html.
[28] C.C.Liebe, J.L. Jørgensen: Algorithms Onboard the Oersted Micro Satellite Stellar Compass, SPIE Proceedings Vol. 2810, Denver 1996, p. 239-251.
[29] C.C.Liebe: Star Trackers for Attitude Determination, IEEE AES Magazine June 1995, p.10-16.

11. BIOGRAPHIES

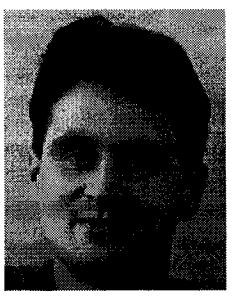

Dr. Carl Christian Liebe received a M.S.E.E. in 1991 and a Ph.D. in 1994 from the Department of Electro-physics, Technical University of Denmark. Since 1997, he has been a member of the technical staff in the Machine Vision and Tracking Sensors Group at the Jet Propulsion Laboratory, California Institute of Technology. His current research interests are new technologies and applications for autonomous attitude determination. He is the cognizant engineer for the future Europa star tracker. He has authored/co-authored more than 25 papers.

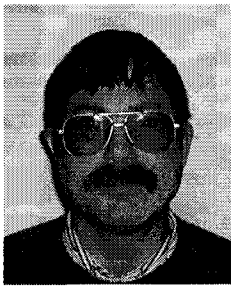

Dr. Bruce Hancock received the B.S.E.E. degree from the California Institute of Technology in 1979, and the M.S.E.E. and Ph.D. degrees from the University of California at Santa Barbara in 1982 and 1985, respectively. He joined the Jet Propulsion Laboratory, California Institute of Technology, Pasadena, in 1985, where his work included molecular beam epitaxy of III-V compounds and infrared sensor technology. More recently, he has been involved in electronic parts reliability and radiation effects. He is currently a member of the Advanced Imager and Focal Plane Technology group, where is investigating radiation effects in active pixel sensors.

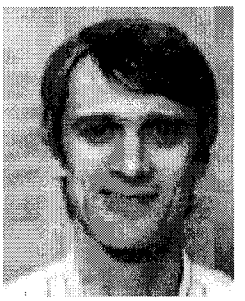

Dr. J. Martin Ratliff holds a Ph.D. in physics from Rice University and is currently Senior technical staff at Jet Propulsion Laboratory. As a member of the Natural Space Environments Group in JPL's Office of Engineering and Mission Assurance, Dr. Ratliff works with spacecraft engineering and science teams to identify and design for missions' relevant environment hazards. This work includes analyses of environments' effects on spacecraft, and measures for mitigating these effects, particularly in the area of charged-particle radiation.

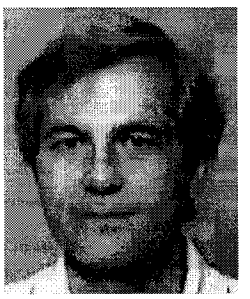

Jim Alexander received an A.B. from U.C. Berkeley and an M.A. and C.Phil from UCLA. Since 1983 he has been heavily involved at JPL in star tracker and scanner testing, analysis, requirements, scene simulation, calibration, algorithm design and implementation for missions as the Astro-1 shuttle experiment, Mars Pathfinder, and the Cassini.

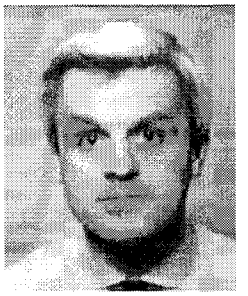

W. John Walker received the B.Sc. degree in Electrical and Electronic Engineering from Queen's University, Belfast, Northern Ireland in 1980 and the M.S. degree in Aeronautics and Astronautics from MIT in 1990. His previous employers include GEC Marconi and Litton

Guidance & Control. Since 1990, he has been a member of technical staff at the Jet Propulsion Laboratory in Pasadena, California, where he has contributed to the design and integration of the attitude control system for the Cassini Mission to Saturn and the Europa Orbiter spacecraft. He is currently involved with the development of real-time control systems for the Space Interferometry Mission.

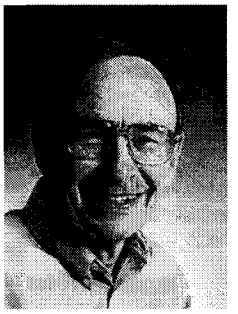

Allan Eisenman holds both bachelor and master of science degrees in electrical engineering from the University of California at Los Angeles. His extensive experience in aerospace engineering includes video display design, analog and digital circuit design, infrared systems engineering, spacecraft science imaging design, complex multi-functional visual and IR focal plane development, space borne video tracking systems, pioneering development of CCD star trackers for spacecraft, celestial sensor development and real sky characterization. Mr. Eisenman is employed at the Jet Propulsion Laboratory in Pasadena, California, as a Senior Staff engineer where he is engaged in the development of advanced celestial and target tracking sensors for Earth-orbiting and interplanetary spacecraft.

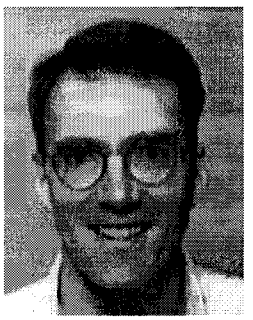

Jeffrey Mellstrom received the B.S.E.E. and M.S.E.E degrees from the University of Minnesota and Rensselaer Polytechnic Institute, respectively. He has worked in military and commercial businesses at General Electric. Since 1988, he has worked in several positions at JPL. He has worked in JPL's Deep Space Network on antenna pointing, hardware design, modeling electromechanical systems, simulation, fault detection and identification, and predictive maintenance. Since 1994, he has worked on flight projects at JPL. He has developed environmental simulations, on-board autonomous functions for the TOPEX spacecraft, and performed system engineering on Mars Pathfinder. He is currently the avionics system engineer for the Europa Orbiter spacecraft.

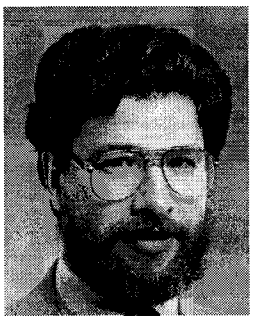

Dr. Gary Swift. Biography not available at this time.

Dr. Wadsworth is a Principal Member of the Engineering Staff in JPL's Space Instruments Implementation Section. For the last two years, he has been employed at JPL where he serves as the technical lead for advanced CCD development and imager characterization activities. At JPL Dr. Wadsworth has been responsible for developing several new state-of-the-art CCD imagers. Recently he has demonstrated a novel imaging methodology known as Hybrid Imaging Technology (HIT), which merges the superior imaging performance of the CCD with the low power and system integration capability of CMOS. His previous thirteen years of experience in optoelectronics at such industry leaders as Texas Instruments and General Electric has led to the development of numerous detectors and imagers for infrared, visible, ultraviolet, and x-ray detection. In addition, his work in CMOS mixed signal design at Texas Instruments led to the development and production of a commercial 10-bit analog-to-digital converter that holds the current industry record for low power, high speed, conversion. Dr. Wadsworth has published over a dozen reviewed papers in the field of optoelectronics and holds eleven patents in this area.